ACS OMEGA

Article

Cite This: ACS Omega 2018, 3, 17416−17424

http://pubs.acs.org/journal/acsodf

Synthesis, Characterization, Swelling, and Metal Uptake Studies of Aryl Cross-Linked Chitosan Hydrogels

Mahir Timur* and Ahmet Paşa

Altınözü Vocational School, Mustafa Kemal University, 31060 Antakya, Hatay, Turkey

Supporting Information

ABSTRACT: Today, many chemical modifications are being made to increase the utilization of chitosan and to make the best use of it. In this study, four novel cross-linked chitosan derivatives in the form of hydrogel (CS-L1 CS-L2, CS-L3, and CS-L4) were prepared by the condensation of chitosan with anisole-based phenolic and nonphenolic aromatic dicarbonyls. Structural analyses were performed by elemental analysis (C, H, N), scanning electron microscopy, Fourier transform infrared, ^{13}C-CP/MAS (cross-polarization, magic angle spinning) nuclear magnetic resonance, powder X-ray diffraction, and thermogravimetric analysis techniques. Metal ion uptake capacities were studied for selected transition-metal cations in aqueous medium. The amount of metal ions was determined by microwave plasma-atomic emission spectroscopy. In addition, the swelling behaviors were investigated at different temperatures (25 and 37 °C) and at different pH values (3, 7, and 10). The order of the selectivity of cross-linked chitosan derivatives toward metal ions was found to be Cu(II) > Cd(II) > Fe(II) > Co(II) > Ni(II). The results showed that the derivatives exhibited the property of hydrogel and suggest that they could be applied in many areas such as metal removing, water removing, and biological applications.

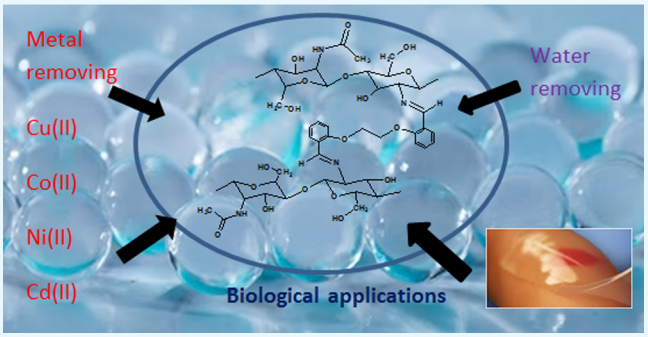

1. INTRODUCTION

Cross-linked polymers with the ability to swell by holding more solvent than 20% of their mass are termed xerogel. When the solvent is water, these cross-linked structures take the name of hydrogel.[1] Hydrogels are physically or chemically cross-linked hydrophilic polymer matrixes that swell by absorbing large amounts of water (or biological fluids) but do not dissolve (in the short term) in water.[2,3]

Among the biopolymers, chitosan is one of the most abundant on earth, thus having great potential in hydrogel preparation.[4] A lot of novel chitosan hydrogels have been obtained by cross-linking over hydroxyl and amino groups of chitosan.[5] Chitosan biopolymer is an amino polysaccharide which is biocompatible, biodegradable, nontoxic, and also antimicrobial. It is open to chemical and mechanical modification in order to gain new features and functions.[6] Today, many new cross-linkers are synthesized and new cross-linked chitosan derivatives are prepared to improve these properties of chitosan.

Biopolymer-based hydrogels have a wide range of applications in the food, pharmaceutical, and biomedical industries because of their biocompatibility and biodegradability.[7] Because of the ability of the hydrogels to swell by holding water in the aqueous medium, they are used in adsorption areas such as manufacturing hygiene products,[8] contact lenses, wound dressings,[7] tissue engineering,[9] water purification, heavy metal removal,[10] controlled drug release,[11] agricultural,[12] ion-exchange applications, chromatographic applications, solvent extraction, removal of water from industrial wastes containing petroleum and oil, and prevention of corrosion.[13]

Derivatization of chitosan can increase the complexation capacity of chitosan with metals, which enhances the adsorption properties of chitosan.[14] In this sense, Schiff base-chitosan derivatives can be used in analytical and environmental applications as a potential metal complex and in organic syntheses as a catalyzer.[15−17]

It is important to examine swelling properties in the characterization of cross-linked polymers that exhibit swelling behavior. For this purpose, it must first be created in the swelling curves. Swelling curves are formed by monitoring changes in the mass or volume of the polymer containing the appropriate solvent over time.[18]

In this study, it was aimed to synthesize chitosan derivatives in the form of hydrogel, which are insoluble in water, can retain more metal, and have phenolic group for biological applications. For this purpose, four cross-linked chitosan derivatives were synthesized by using aromatic dialdehyde and diketones as the cross-linking agent. Derivatives were characterized by spectroscopic methods. In addition, metal ions uptake capacities and swelling behaviors of cross-linked chitosan derivatives were investigated.

Received: August 2, 2018
Accepted: December 3, 2018
Published: December 17, 2018

DOI: 10.1021/acsomega.8b01872
ACS Omega 2018, 3, 17416−17424

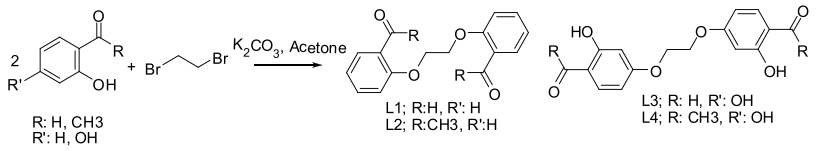

Figure 1. Synthesis route of dialdehydes and diketones.

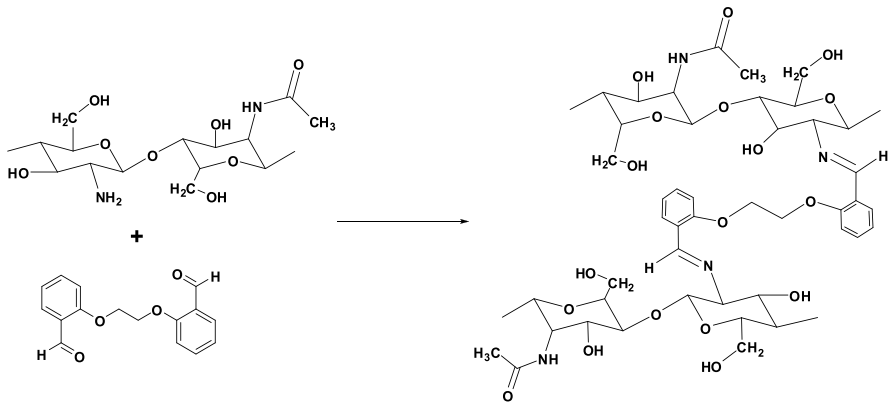

Figure 2. Synthesis of cross-linked chitosan derivative (CS-L1).

2. MATERIALS AND METHODS

2.1. Materials. Chitosan was purchased from Sigma-Aldrich with a molecular weight of 310−375 kDa (high molecular weight) and 75% degree of deacetylation. Salicylaldehyde, acetophenone, 2,4-dihydroxyacetophenone, diethyl amine, 1,2-dibromoethane, and acetic acid were purchased from Merck. 2,4-Dihydroxybenzaldehyde was purchased from Roth. Stock solutions of $Cu(CH_3COO)_2 \cdot 1H_2O$, $Co(CH_3COO)_2 \cdot 4H_2O$, $NiCl_2 \cdot 6H_2O$, $Cd(CH_3COO)_2 \cdot 2H_2O$, and $FeSO_4 \cdot 7H_2O$ were prepared by dissolving the appropriate amount of metal(II) salt (analytical grade) in deionized water. All solvents were of reagent-grade quality, and they were obtained from commercial suppliers and were purified before use by a well-known distillation method.

Melting points were recorded on Electrothermal IA9200. Elemental analyses of the compounds for C, H, and N were carried out with LECO-CHNS-932. The samples were analyzed with a Fourier transform infrared spectrophotometer PerkinElmer spectrum two, equipped with a diamond-tipped attenuated total reflection (ATR) accessory. The analysis region ranged from 400 to 4000 cm^{-1}. ^{13}C NMR spectra were obtained by a Bruker Superconducting FT/NMR Spectrometer Avance TM 300 MHz WB with CP/MAS technique (cross-polarization, magic angle spinning). The cell was cleaned three times with acetone after each spectrum was acquired. Thermogravimetric analyses (TGA) of the samples were performed with a Mettler Toledo thermal analyzer under nitrogen atmosphere and heated from 20 to 800 °C at a heating rate of 10 °C min^{-1}. The X-ray diffraction (XRD) patterns of samples were recorded at room temperature on a Rigaku System RadB X-ray diffractometer, using monochromated Cu Kα radiation in the range 2°−40° (2θ), at 25 °C. Morphological analysis of images obtained was carried out by scanning electron microscopy (SEM), JEOL 5500. Metal analysis was carried out by microwave plasma-atomic emission spectroscopy (MP-AES): Agilent 4100 in a solution prepared by decomposition of the complex with HNO_3 followed by dilution with distilled water.

2.2. Methods. *2.2.1. General Procedure for the Synthesis of Dialdehydes and Diketones (L1−L4).* Dialdehydes and diketones exist in the literature, and they (L1−L4) were synthesized according to the literature.[19] The proposed structures of dialdehyde and diketone are given in Figure 1.

To a round-bottom flask, the corresponding phenol derivative (12 mmol) was added in acetone (20 mL) followed by anhydrous K_2CO_3 (20 mmol, 2.78 g), and the flask was dipped into a preheated oil bath (80 °C) and stirred at 80 °C for 15 min. After 15 min, the temperature of the oil bath was raised to 110 °C. Then, to the hot reaction mixture, 1,2-dibromoethane (5 mmol) was added in one portion. The resulting reaction mixture was stirred at 110 °C for 12 h, and after this period, the flask was allowed to cool to room temperature. Next, the reaction mixture was poured onto crushed ice (50−75 g). Finally, the solid compound (dicarbonyl) that formed was filtered through a filtration funnel and was purified by rapid column chromatography followed by crystallization from $CHCl_3$−petroleum ether. The prepared compounds were characterized by their melting points and Fourier transform infrared (FT-IR−ATR) spectra.[19]

2.2.1.1. 1,2-Bis-(2-formylphenoxy)ethane (L1).[20] Colorless needles, mp 128−129 °C (lit. 128−130 °C), yield (0.9 g, 33%) IR (ATR), ν_{max}/cm^{-1}: 1061, 1189, 1240, 1288, 1398, 1450, 1483, 1596, 1664, 1683, 2866.

2.2.1.2. 1,2-Bis-(2′-acetylphenoxy)ethane (L2).[20] Colorless, mp 126 °C (lit. 126 °C), yield (0.72 g, 24%) IR (ATR), ν_{max}/cm^{-1}: 1045, 1133, 1154, 1227, 1064, 1107, 1247, 1289, 1351, 1447, 1469, 1485, 1592, 1663, 2949.

2.2.1.3. 1,2-Bis(4′-formyl-3′-hydroxyphenoxy) Ethane (L3).[21] Colorless needles, mp 167−168 °C (lit. 168 °C), yield (0.69 g, 23%) IR (ATR), ν_{max}/cm^{-1}: 1039, 1100, 1173, 1225, 1253, 1385, 1433, 1498, 1598, 1622, 1644, 2931, 3254.

2.2.1.4. 1,2-Bis(4′-acetyl-3′-hydroxyphenoxy) Ethane (L4).[22] Colorless, mp 172−173 °C (lit. 174 °C), yield (0.69 g, 21%) IR (ATR), ν_{max}/cm^{-1}: 986, 1013, 1067, 1135, 1191, 1231, 1253, 1331, 1368, 1427, 1504, 1594, 1622, 2929, 3400.

DOI: 10.1021/acsomega.8b01872
ACS Omega 2018, 3, 17416−17424

2.2.2. Synthesis of Cross-Linked Chitosan Derivative (CS-L1). Chitosan derivatives were prepared according to the literature.[23] Chitosan (1.0 g) was stirred in a 100 mL 1% acetic acid solution at 60 °C for 1 h to obtain a homogeneous mixture. To the resulting chitosan solution, 50 mL of ethanolic solution of L1 (1.57 g, 5.83 mmol) was added and stirred under reflux for 12 h. Then, the mixture was cooled to room temperature, and at the end, a precipitate was obtained in the form of gel by adding 1 M $NaHCO_3$. The gel was filtered and dried in a vacuum oven at 70 °C. The prepared gel was purified with Soxhlet extraction by using ethanol as the solvent.

The synthetic route is shown in Figure 2. The formation of imine bond (C═N) as a result of the reaction of amine group (from chitosan) with the carbonyl group (from aldehyde) was given the resultant desired cross-linked product CS-L1.

The cross-linked chitosan derivatives were synthesized according to the same procedure of CS-L1 by using 1.73 g L2, 1.76 g L3, and 1.92 g L4. The prepared cross-linked chitosan derivatives were coded as CS-L2 (Figure S1), CS-L3 (Figure S2), and CS-L4 (Figure S3), respectively.

2.2.3. Metal Ion Uptake Studies. At acidic pH (3.5−5.5), the complex formation between the metal ion and the chitosan derivative reduces as the free-amine groups of the chitosan are protonated. Amino groups are present as free amines at pH 6.5−7.0 and the metal retention capacity of the chitosan derivative increases.[24] A series of transparent and stable hydrogels is obtained by mixing chitosan with various metal ions at appropriate pH values.[25]

The metal ion uptake studies were performed, at 25 ± 0.1 °C in pH 6 buffered medium on an orbital shaker for 3 h, by shaking 50 mg of the derivative in 50 mL of 100 ppm Cu(II), Co(II), Ni(II), Cd(II), and Fe(II) solutions (metal/derivative ratios were prepared as 100 mg metal/1 g derivative). The pH of the solution was adjusted using acetic acid/sodium acetate for pH 6.[26] After that, the suspension was filtered and diluted (1:20), and the amounts of metal ions remaining in the solution were determined by MP-AES.

The metal ion uptake capacities of chitosan derivatives in mg/g are calculated by the following eq 1

$$C = W_a/W_p \tag{1}$$

where C is the metal holding capacity in mg/g, the amount of metal retained as W_a (mg), and W_p is the mass of the derivative in grams.

2.2.4. Swelling Studies. The swelling experiments of the cross-linked chitosan derivatives were carried out in the water medium at 25 and 37 °C and pH 3.0, 7.0, and 10.0. NaOH (0.1 M) and 0.1 M HCl were used to adjust the pH solutions. The samples were weighed at a sensitivity of 0.1 mg and placed in an aqueous environment sensitive to ±0.1 °C. When the derivative was left in the solution, t = 0 was taken and it removed from the water at certain time intervals were dried and weighed. After 180 min, the experiment was terminated because of the swelling slowed.

Swelling % (S %) is calculated by the following eq 2

$$S\,\% = \frac{W_t - W_o}{W_o} \times 100 \tag{2}$$

where S %, W_t, and W_o are the percent of swelling, weight at different times, and initial weight of the sample, respectively.[27]

2.2.5. Swelling Kinetics Studies. For extensive swelling of polymers, the following second-order kinetics relation can be used[28]

$$\frac{t}{s} = A + Bt \tag{3}$$

where t is time, S is swelling at t, $B = 1/S_{max}$ is the inverse of the maximum or equilibrium swelling, $A = 1/kS\ S_{max}^2$ is the reciprocal of the initial swelling rate $[(dS/dt)_0]$ of the hydrogel, and kS is swelling rate constant.

The linear regressions of the swelling curves were obtained by means of eq 3 for the hydrogels in water at different temperatures and pH.

3. RESULTS AND DISCUSSION

3.1. Solubility. It is well-known that chitosan is insoluble in water, organic solvents, and aqueous bases, and it is soluble after stirring in acids such as acetic, nitric, hydrochloric, perchloric, and phosphoric.[29]

As a result of the derivatization of chitosan from amine groups, it is expected that the solubility of chitosan derivatives in comparison to chitosan will decrease because of the decrease of free-amine groups. As a result, it has been observed that cross-linked chitosan derivatives are not soluble in aqueous acid or basic solutions, but depending on the cross-linking ratio, low cross-linked CS-L2 and CS-L4 derivatives are dispersed in these solutions in time.

3.2. Elemental Analyses. The C, H, and N elemental analysis results and C/N ratio values of the prepared cross-linked chitosan derivatives are given in Table 1.

Table 1. C, H, and N Elemental Analysis Results of Cross-Linkers and Hydrogels[a]

	% C	% H	% N	C/N	DS	*a*	*n*
chitosan (CS)	40.95	6.96	7.41	5.53			
L1	71.79	5.28					
L2	72.71	5.98					
L3	63.48	4.64					
L4	65.72	5.56					
CS-L1	45.64	4.74	3.12	14.63	0.65	1	14
CS-L2	43.43	5.89	5.57	7.80	0.15	1	15
CS-L3	32.43	4.61	1.91	16.98	0.82	1	14
CS-L4	34.74	5.52	4.29	8.10	0.17	1	15

[a]DS: degree of substitution; *a*: the number of nitrogen; *n*: the number of carbon.

The elemental analysis results of the synthesized chitosan derivatives showed an increase in the C % and H % values and a decrease in the N % values due to the dicarbonyl compound (which does not contain nitrogen atoms) entering the reaction. These changes were more easily detected by calculating C/N ratios. When the C/N ratios are examined, it is seen that the C/N ratios of synthesized cross-linked chitosan derivatives are higher than those of chitosan. These results are considered to be important evidence showing that new chitosan derivatives have been obtained.

The number of carbonyl attached to each NH_2 group in the chitosan was calculated as the degree of substitution (DS) by the following eq 4:[30]

$$DS = \frac{a(C/N)_m - (C/N)_o}{n} \tag{4}$$

DOI: 10.1021/acsomega.8b01872
ACS Omega 2018, 3, 17416−17424

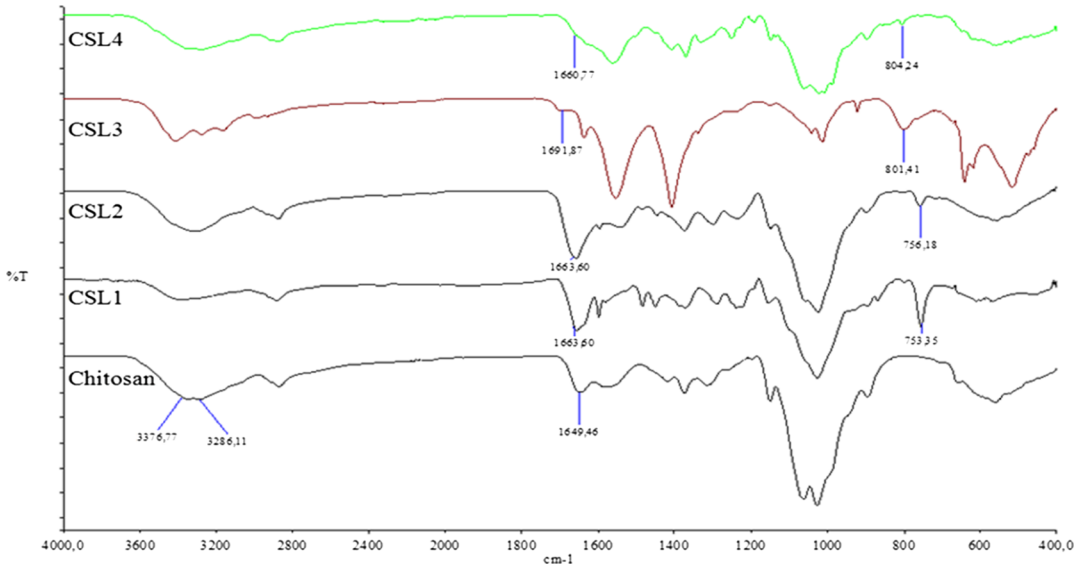

Figure 3. FT-IR spectra of chitosan and derivatives.

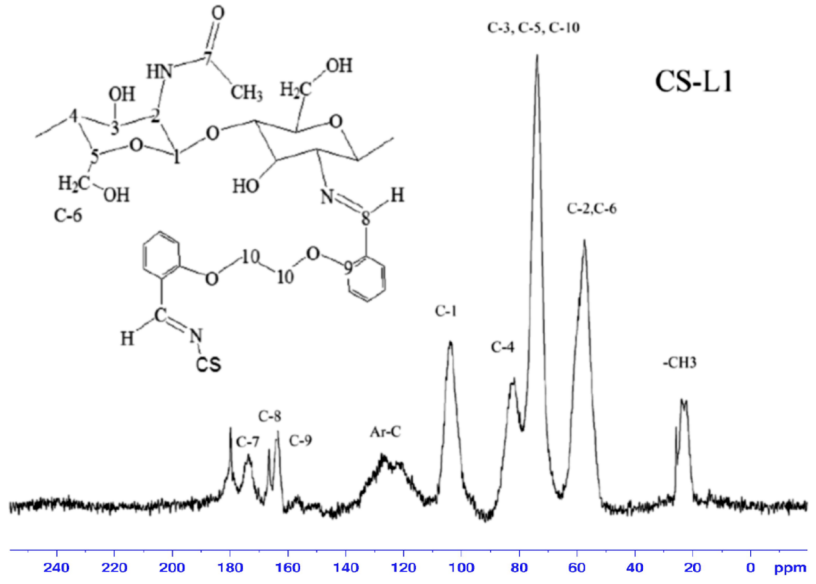

Figure 4. ^{13}C CP-MAS NMR spectrum of CS-L1.

$(C/N)_m$ is the modified chitosan C/N ratio, $(C/N)_o$ is the initial chitosan C/N ratio, and "*a*" and "*n*" are the number of nitrogen and carbon contained after the chitosan has been modified, respectively. The DS of chitosan derivatives is given in Table 1. Because the activity of aldehyde in Schiff base formation is higher than that of ketones, maximum substitution was observed in the aldehyde derivatives. The cross-linking sequence is obtained as CS-L3 > CS-L1 > CS-L4 > CS-L2.

3.3. FT-IR Spectra. In order to characterize the hydrogels, a spectrum of pure chitosan was also recorded. The main bands appearing in the IR spectra of chitosan spectrum, vibrations of OH groups in the region of 3500−3000 cm^{-1}, which are overlapped to the stretching vibration of N−H, the vibrations of carbonyl bonds (C═O) of the amide group in the range of 1680−1480 cm^{-1}, vibrations of etheric CO in the range from 1160 to 1000 cm^{-1}, and the bands near 1080−1025 cm^{-1} are attributed to etheric CO of the ring, and the peak at ∼890 cm^{-1} corresponding to wagging of the saccharide structure of chitosan appears.[31]

Comparing the spectrum of chitosan (CS) with the spectra of hydrogels, we can observe that they differ from each other. In the spectra of chitosan derivatives, some bands although broadened and shifted, some new bands were observed at the range of 1300−1600 cm^{-1} (Figure S4). These new bands can be attributed to the vibrational modes of C═N, C═C, and C−H groups of the Schiff base moities.[32]

In the IR spectra of hydrogels, the NH stretching vibrations of chitosan disappeared and −OH stretching vibrations were observed as a broad band in the range from 3000 to 3600 cm^{-1}, and the 1651 cm^{-1} band shifted to 1663 cm^{-1} (CS-L1), 1663 cm^{-1} (CS-L2), 1691 cm^{-1} (CS-L3), and 1660 cm^{-1} (CS-L4), which can be attributed to the C═N of Schiff base, respectively. In addition, for CS-L1 and CS-L2, the disubstitute benzene peak was observed at 753 and 756 cm^{-1}, whereas the trisubstitue benzene peak for CS-L3 and CS-L4 was observed at 801 and 804 cm^{-1}, respectively (Figure 3).

3.4. ^{13}C CP-MAS Solid-State NMR Analysis. In previous studies, chitosan with a degree of acetylation of 75% was given

DOI: 10.1021/acsomega.8b01872
ACS Omega 2018, 3, 17416−17424

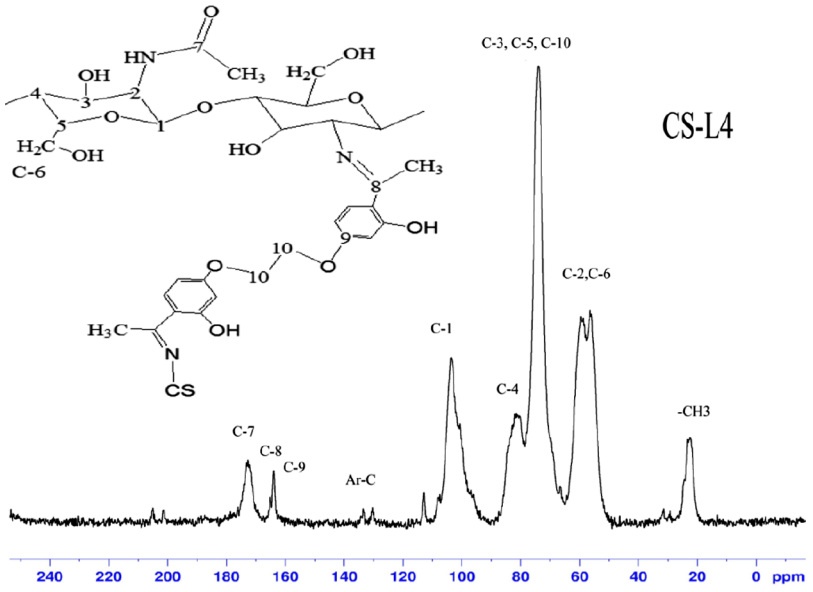

Figure 5. ^{13}C CP-MAS NMR spectrum of CS-L4.

^{13}C CP-MAS solid-state NMR chemical shift values at 23 ppm (−CH3), 58 ppm (C2), 61 ppm (C6), 76 ppm (C5, C3), 85 ppm (C4), 106 ppm (C1), and 174 ppm (C═O), respectively.[33] As compared with chitosan, new peaks were observed from 110 to 140 ppm (aromatic carbons), 70 ppm (C-10; overlapped signal with chitosan C3, C4, C5 carbons), 163 ppm (C-9; benzene carbon adjacent to etheric oxygen atom), 166 ppm (C-8; azomethine carbon), and 180 ppm (free carbonyl carbon) in the spectrum of derivatives. The formation of new peaks confirms the formation of the cross-linked chitosan derivatives (Figures 4, 5, S5, and S6).

^{13}C NMR can be used as a quantitative tool.[34] The intensity of the new peaks varied in direct proportion with cross-linking. As the cross-linking decreases, the peak intensity was decreased. Elemental analysis results showed that cross-linking in CS-L2 and CS-L4 was less than in CS-L1 and CS-L3, and also in the C NMR spectra, the peak intensity of CS-L2 and CS-L4 was observed to be lower than that of CS-L1 and CS-L3. When the ^{13}C NMR peak intensities of the derivatives are considered, the peak intensities of C NMR are in agreement with the results of elemental analysis.

3.5. Morphology. One of the most commonly used methods for understanding the surface properties and porosity of polymeric samples is the SEM method.[35]

The difference in structural morphology between chitosan and CS-L1, CS-L2, CS-L3, and CS-L4 is also supported by the difference in SEM images. SEM results show that derivatives different from chitosan were synthesized. SEM images of chitosan and chitosan derivatives are shown in Figure 6.

Chitosan derivatives exhibit a wider three-dimensional rough structure compared to the smooth surface of chitosan.[36]

3.6. XRD (Powder XRD) Analysis. It was previously reported that CS exhibits two sharp crystalline peaks at 2θ = 10° and 2θ = 20°, which attributed to intermolecular and intramolecular hydrogen bonds of chitosan, respectively.[16,37] It is known that the intermolecular and intramolecular hydrogen bondings formed between amino group and a hydroxyl group stabilize the crystalline structure of chitosan.

Crystallinity decreases by the deformation of some intermolecular and intramolecular hydrogen bonds because

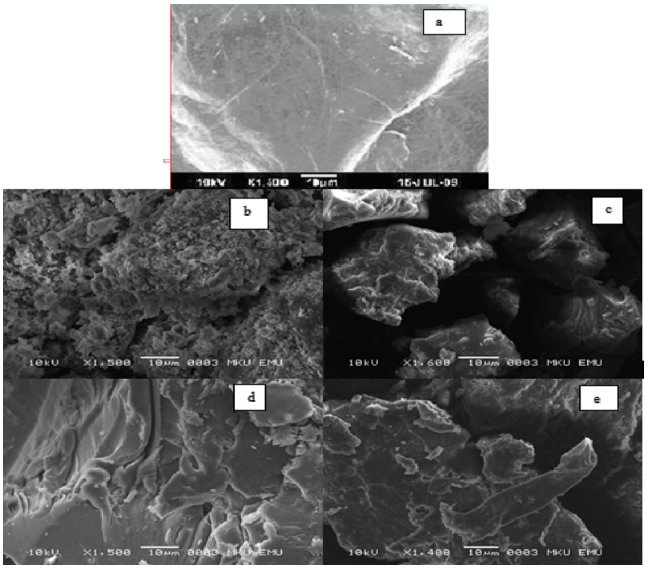

Figure 6. Scanning electron micrographs of chitosan (a), CS-L1 (b), CS-L2 (c), CS-L3 (d), and CS-L4 (e).

of both the decreasing free-amino group and formation of steric hindrance after cross-linking.[38−40] Chitosan derivatives with amorphous structure can be used in biomedical applications.[36]

In the XRD pattern of derivatives, the intensity of peaks decreased and broadening of the peaks was observed when compared with the free chitosan. These results suggest that the derivatives have a less crystalline and more amorphous structure than the pure chitosan (Figure S7).

According to XRD results, the peak intensity of the dialdehyde derivatives CS-L1 and CS-L3 was decreased more and the peaks were broadened more when compared with the diketone derivatives CS-L2 and CS-L4. The more deformation in the crystal structure has shown that more cross-linking takes place in the chitosan polymer.

3.7. Thermogravimetric Analysis. The thermal properties of the derivatives were investigated by TGA techniques

DOI: 10.1021/acsomega.8b01872
ACS Omega 2018, 3, 17416−17424

under a nitrogen atmosphere. Chitosan exhibits a one-step degradation reaction in the nitrogen environment. TGA thermograms of derivatives are shown in Figure S8.

It is well-known that chitosan has two mass loss stages: water elimination and decomposition. These stages are observed at 40−100 °C range and 280−400 °C range, respectively.[41] Degradation of Schiff bases occurs at 300−400 °C, and evaporation of the phenolic group occurs above 400 °C.[42] The degradation values of chitosan derivatives were given in Table 2.

Table 2. Degradation Temperature of Derivatives

	1. degradation range (°C) (weight loss %)	2. degradation range (°C) (weight loss %)	2. degradation temperature (°C)	carbon residue % (at 600 °C)
chitosan	50−150(∼10)	150−600(∼59)	319	30, 99
CS-L1	75−156(∼15)	236−600(∼44)	291	40, 79
CS-L2	50−250(∼10)	259−600(∼53)	301	37, 15
CS-L3	50−225(∼11)	225−400(∼36)	264	44, 59
		400−600(∼9)	468	
CS-L4	50−225(∼5)	225−400(∼38)	284	43, 51
		400−600(∼13)	479	

Weight loss in the range of 50−200 °C observed by means of the loss of water. In addition to the loss of water, derivatives also display other significant weight losses in the region 250−350 °C, attributable to the decomposition of Schiff base and chitosan chains. On the other hand, for CS-L3 and CS-L4, another weight loss was observed at 450−600 °C range, which attributed to the evaporation of phenolic OH.

When the results of CS-L compared with the results of the chitosan in terms of the thermal behaviors, there are many important differences and can be observed due to the interaction between chitosan and dicarbonyls.

As a result, all derivatives exhibited lower final degradation temperature than chitosan due to the derivatization. According to the results, chitosan derivatives are less thermally stable than chitosan. This instability can be attributable to deterioration of the crystallinity of chitosan by Schiff base formation.[32]

3.8. Metal Ion Uptake Results. According to the MP-AES analysis, the amount of uptake Cu(II), Co(II), Ni(II), Cd(II), and Fe(II) for per gram derivative was given in Table 3.

The capacities of hydrogels for Cu(II) ions were found as CS-L1 (84.0 mg g^{-1}), CS-L2 (71.8 mg g^{-1}), CS-L3 (59.6 mg g^{-1}), and CS-L4 (64.0 mg g^{-1}). All hydrogels exhibited a higher uptake capacity for Cu(II) ions than the other metal ions used in the study. According to obtained data, metal uptake capacity of the hydrogels was found as CS-L1 > CS-L2 > CS-L4 > CS-L3. As a result, hydrogels showed selectivity toward Cu(II), Fe(II), and Cd(II) ions.

The cross-linking sequence was in the form of CS-L3 > CS-L1 > CS-L4 > CS-L2, whereas the metal capture sequence was CS-L1 > CS-L2 > CS-L4 > CS-L3, depending on the cross-linking ratio and bonding geometry.

The degree of swelling of hydrogel decreases, as the cross-linking increases and the structure becomes tighter. In this case, the hydrogel is less swollen, most of the metal ions are not infiltrated into the inner part of the hydrogel, and metal uptake happens only on the surface of the hydrogels.[43] In previous studies, the Cu(II) metal uptake capacity of glutaraldehyde cross-linked epoxyaminated chitosan as 51.75 mg/g[44] and glutaraldehyde cross-linked chitosan nanofibers as 72 mg/g[45] had been found. The metal retention capacity of the synthesized derivatives was found to be higher than or close to these values.

3.9. Swelling Behaviors. *3.9.1. Percent Swelling.* At equilibrium, hydrogel has the greatest swelling value. With the help of the obtained data, swelling kinetics of network polymers can be determined by calculating values such as equilibrium percent swelling, initial swelling rate, swelling rate constant, and theoretical equilibrium percent swelling.[46]

Percent swelling rate (S %) was calculated according to eq 2. The values of percent swelling of hydrogels are given in Table 4 (Figure S9−S16, see Supporting Information).

Table 4. Percent Swelling Rate (S %) of Derivatives at Different Temperatures and pH

	25 °C (S %)			37 °C (S %)		
	pH 3	pH 7	pH 10	pH 3	pH 7	pH 10
CS-L1	497	562	711	368	557	437
CS-L2	115	110	165	93	107	212
CS-L3	28	173	196	28	159	202
CS-L4	100	159	123	84	148	132

In chitosan films, as the cross-linker concentration increased, the water retention capacity and the release of active substances from the film decrease.[47]

The degree of swelling varies with the pH for all hydrogels. Partial acid and basic hydrolysis affected the swelling behavior of the derivatives. Swelling of hydrogels occurs by hydrogen bond formation. As the hydrophilic groups increase, the hydrogen bond formation increases. The OH groups present in the synthesized hydrogels and the free NH_2 groups remaining unreacted perform the swelling process by hydrogen bonding with water. In the acidic environment, as these functional groups are protonated, less hydrogen bonding and less swelling occurs compared to the basic environment.

We have found that the swelling behavior of hydrogels strongly depends on the pH and the degree of its swelling increases with the increase of pH.

The highest swelling value was observed in CS-L1 because of its porous structure. Water retention generally occurred in neutral and basic medium.

Table 3. Amount of Metal Held by Derivatives

	Cu(II)		Cd(II)		Fe(II)		Co(II)		Ni(II)	
	mg/g	ppm	mg/g	ppm	mg/g	ppm	mg/g	ppm	mg/g	ppm
CS-L1	84.0	84 000	83.8	83 800	80.6	80 600	78.4	78 400	78.0	78 000
CS-L2	71.8	71 800	57.2	57 200	56.0	56 000	39.0	39 000	20.2	20 200
CS-L3	59.6	59 600	49.4	49 400	59.2	59 200	29.8	29 800	9.2	9200
CS-L4	64.0	64 000	60.8	60 800	59.8	59 800	33.6	33 600	12.2	12 200

DOI: 10.1021/acsomega.8b01872
ACS Omega 2018, 3, 17416−17424

As the temperature increases, the water retention rate is lower than the low temperature because of increased solubility in the hydrogel.

3.9.2. Equilibrium Water Content. In cross-linked polymers, after a certain time after having been exposed to the solvent environment, the rate at which the solvent enters and leaves the structure becomes equal and the balance is reached. At this point, hydrogel has the greatest swelling value.

For hydrogels in equilibrium with solvent, the equilibrium water content (EWC) is calculated by eq 5[48]

$$\mathrm{EWC} = \frac{W_e - W_o}{W_e} \quad (5)$$

In the equation, W_e is the equilibrium (swollen) polymer mass and W_o shows the mass of dry polymer.

The equilibrium liquid content is a parameter which is calculated for the hydrogel in this case and is very important for biocompatibility. For hydrogels, EWC values greater than 0.60 are indicative of potential biocompatibility. The EWC values were given in Table 5.

Table 5. EWC Values of Derivatives

	pH					
compound	pH 3	pH 7	pH 10	pH 3	pH 7	pH 10
CS-L1	0.81	0.72	0.77	0.79	0.74	0.81
CS-L2	0.26	0.28	0.24	0.48	0.52	0.68
CS-L3	0.22	0.68	0.69	0.22	0.62	0.67
CS-L4	0.51	0.60	0.62	0.46	0.60	0.57

Most of the derivatives were found to have an EWC value greater than 0.60 at different pH ranges and temperatures. According to these results, all derivatives exhibited hydrogel properties.

3.9.3. Swelling Kinetics Studies. The initial swelling rate, the swelling rate constant, and the values of theoretical equilibrium swelling of the hydrogel were calculated from the slope and the intersection of the lines, respectively. The results are presented in Table 6 (Figures S17−S40, see the Supporting Information)

4. CONCLUSIONS

In this work, new cross-linked chitosan hydrogels were synthesized by the formation of Schiff base. Elemental analysis (C, H, N), SEM, FT-IR, ^{13}C-CP/MAS NMR, powder XRD, and TGA technique data support that the chitosan is cross-linked.

When swelling rates are taken into account, cross-linking was more often observed in dialdehyde cross-linked chitosan derivatives. Also, this is supported by the DS, ^{13}C CP-MAS solid-state NMR, and XRD analysis. Increasing the degree of cross-linking of the system will result in a stronger gel, and a higher degree of cross-linking creates a more brittle structure.

In the swelling experiments, the experimental results and the theoretical data are in agreement with one another. Although hydrogels generally swelled faster at 37 °C, less swelling was observed with increasing temperature because of increased solubility. For all derivatives, the highest initial swelling rate was found at pH 10 for both 25 and 37 °C.

EWC values of some hydrogels are close to the percent water content values of the body, 0.60 (or 60%). Accordingly, most hydrogels exhibit liquid contents similar to living tissues.[49]

Generally, the metal uptake order is Cu(II) > Fe(II) > Cd(II) > Co(II) > Ni(II). As a result of this study, besides being the most Cu(II), it can be said that all derivatives showed selectivity toward Cu(II), Fe(II), and Cd(II) ions.

Although maximal cross-linking is observed in CS-L1 and CS-L3, maximum metal retention and swelling were found in CS-L1 because of its porous structure (Figure 6). A result of high swelling of CS-L1 facilitates diffusion of metal ions to the CS-L1 interior. The least metal retention is found in CS-L3 because CS-L3 is highly cross-linked and its structure is more rigid.

■ ASSOCIATED CONTENT

Supporting Information

The Supporting Information is available free of charge on the ACS Publications website at DOI: 10.1021/acsomega.8b01872.

Synthesis of cross-linked chitosan derivative (CS-L2), synthesis of cross-linked chitosan derivative (CS-L3),

Table 6. Initial Swelling Rate, Swelling Rate Constant, and Values of Theoretical Equilibrium Swelling of CS-L1−CS-L4

	25 °C			37 °C		
	pH 3	pH 7	pH 10	pH 3	pH 7	pH 10
			CS-L1			
r_0	27.17	31.45	54.05	94.34	169.49	64.51
S_{max}	555.55	625.00	769.23	370.37	526.31	454.55
$k_s \times 10^{-4}$	0.88	0.81	0.91	6.87	6.12	3.12
			CS-L2			
r_0	7.14	23.42	33.22	3.64	28.90	40.65
S_{max}	114.94	111.11	166.67	92.59	108.68	217.39
$k_s \times 10^{-4}$	5.49	18.90	12.00	4.24	24.50	8.60
			CS-L3			
r_0	1.70	8.38	15.06	1.81	9.04	28.09
S_{max}	30.49	185.00	204.08	28.90	178.57	208.33
$k_s \times 10^{-4}$	18.30	2.44	3.61	21.70	2.83	6.47
			CS-L4			
r_0	13.77	16.31	25.00	11.69	15.15	23.31
S_{max}	101.01	163.93	128.20	84.75	156.25	133.33
$k_s \times 10^{-4}$	13.50	6.07	15.20	16.30	6.21	13.10

DOI: 10.1021/acsomega.8b01872
ACS Omega 2018, 3, 17416−17424

synthesis of cross-linked chitosan derivative (CS-L4), expanded FT-IR spectra of chitosan and derivatives (1300−1600 cm^{-1}), ^{13}C CP-MAS NMR spectrum of CS-L2, ^{13}C CP-MAS NMR spectrum of CS-L3, XRD diffractograms of chitosan and chitosan derivatives, TGA thermograms of derivatives, % swelling values of CS-L1 derivative at 25 °C and different pH values, % swelling values of CS-L1 derivative at 37 °C and different pH values, % swelling values of CS-L2 derivative at 25 °C and different pH values, % swelling values of CS-L2 derivative at 37 °C and different pH values, % swelling values of CS-L3 derivative at 25 °C and different pH values, % swelling values of CS-L3 derivative at 37 °C and different pH values, % swelling values of CS-L4 derivative at 25 °C and different pH values, % swelling values of CS-L4 derivative at 37 °C and different pH values, swelling kinetics curve of CS-L1 at pH 3 and at 25 °C, swelling kinetics curve of CS-L1 at pH 7 and at 25 °C, swelling kinetics curve of CS-L1 at pH 10 and at 25 °C, swelling kinetics curve of CS-L1 at pH 3 and at 37 °C, swelling kinetics curve of CS-L1 at pH 7 and at 37 °C, swelling kinetics curve of CS-L1 at pH 10 and at 37 °C, swelling kinetics curve of CS-L2 at pH 3 and at 25 °C, swelling kinetics curve of CS-L2 at pH 7 and at 25 °C, swelling kinetics curve of CS-L2 at pH 10 and at 25 °C, swelling kinetics curve of CS-L2 at pH 3 and at 37 °C, swelling kinetics curve of CS-L2 at pH 7 and at 37 °C, swelling kinetics curve of CS-L2 at pH 10 and at 37 °C, swelling kinetics curve of CS-L3 at pH 3 and at 25 °C, swelling kinetics curve of CS-L3 at pH 7 and at 25 °C, swelling kinetics curve of CS-L3 at pH 10 and at 25 °C, swelling kinetics curve of CS-L3 at pH 3 and at 37 °C, swelling kinetics curve of CS-L3 at pH 7 and at 37 °C, swelling kinetics curve of CS-L3 at pH 10 and at 37 °C, swelling kinetics curve of CS-L4 at pH 3 and at 25 °C, swelling kinetics curve of CS-L4 at pH 7 and at 25 °C, swelling kinetics curve of CS-L4 at pH 10 and at 25 °C, swelling kinetics curve of CS-L4 at pH 3 and at 37 °C, swelling kinetics curve of CS-L4 at pH 7 and at 37 °C, and swelling kinetics curve of CS-L4 at pH 10 and at 37 °C (PDF)

AUTHOR INFORMATION

Corresponding Author

*E-mail: timur@mku.edu.tr. Phone: +90 505 545 13 72. Fax: +90 326 245 58 67 (M.T.).

ORCID

Mahir Timur: 0000-0001-5914-607X

Notes

The authors declare no competing financial interest.

ACKNOWLEDGMENTS

This work was supported by the Research Fund of Mustafa Kemal University project number: 13220.

REFERENCES

(1) Laftah, W. A.; Hashim, S.; Ibrahim, A. N. Polymer hydrogels: A review. *Polym.—Plast. Technol. Eng.* **2011**, *50*, 1475−1486.

(2) Kopecek, J. Polymer chemistry: swell gals. *Nature* **2002**, *417*, 388−391.

(3) Peppas, N.; Bures, P.; Leobandung, W.; Ichikawa, H. Modular hydrogels for drug delivery. *Eur. J. Pharm. Biopharm.* **2000**, *50*, 27−46.

(4) Boonsongrit, Y.; Mitrevej, A.; Mueller, B. Chitosan drug binding by ionic interaction. *Eur. J. Pharm. Biopharm.* **2006**, *62*, 267−274.

(5) Peng, K.; Tomatsu, I.; Kros, A. Hydrogel-based drug carriers for controlled release of hydrophobic drugs and proteins. *J. Controlled Release* **2011**, *152*, e72−e74.

(6) Jayakumar, R.; Prabaharan, M.; Nair, S. V.; Tokura, S.; Tamura, H.; Selvamurugan, N. Novel carboxymethyl derivatives of chitin and chitosan materials and their biomedical applications. *Prog. Mater. Sci.* **2010**, *55*, 675−709.

(7) Jayakumar, R.; Prabaharan, M.; Sudheesh Kumar, P. T.; Nair, S. V.; Tamura, H. Biomaterials based on chitin and chitosan in wound dressing applications. *Biotechnol. Adv.* **2011**, *29*, 322−337.

(8) Zohuriaan-Mehr, M. J.; Pourjavadi, A.; Salimi, H.; Kurdtabar, M. Protein- and homo poly(amino acid)-based hydrogels with super-swelling properties. *Polym. Adv. Technol.* **2009**, *20*, 655−671.

(9) Lee, K. Y.; Mooney, D. J. Hydrogels for tissue engineering. *Chem. Rev.* **2001**, *101*, 1869−1880.

(10) Li, G.; Du, Y.; Tao, Y.; Deng, H.; Luo, X.; Yang, J. Iron(II) cross-linked chitin-based gel beads: Preparation, magnetic property and adsorption of methyl orange. *Carbohydr. Polym.* **2010**, *82*, 706−713.

(11) Qiu, Y.; Park, K. Environment-sensitive hydrogels for drug delivery. *Adv. Drug Delivery Rev.* **2012**, *64*, 49−60.

(12) Arbona, V.; Iglesias, D. J.; Jacas, J.; Primo-Millo, E.; Talon, M.; Gómez-Cadenas, A. Hydrogel substrate amendment alleviates drought effects on young citrus plants. *Plant Soil* **2005**, *270*, 73−82.

(13) Juang, R.-S.; Shiau, R.-C. Metal removal from aqueous solutions using Chitosan-enhanced membrane filtration. *J. Membr. Sci. Technol.* **2000**, *165*, 159−167.

(14) Wan, M.-W.; Kan, C.-C.; Rogel, B. D.; Dalida, M. L. P. Adsorption of copper (II) and lead (II) ions from aqueous solution on chitosan-coated sand. *Carbohydr. Polym.* **2010**, *80*, 891−899.

(15) Baran, T.; Menteş, A.; Arslan, H. Synthesis and characterization of water soluble O-carboxymethyl chitosan Schiff bases and Cu(II) complexes. *Int. J. Biol. Macromol.* **2015**, *72*, 94−103.

(16) Baran, T.; Açıksöz, E.; Menteş, A. Highly efficient, quick and green synthesis of biarlys with chitosan supported catalyst using microwave irradiation in the absence of solvent. *Carbohydr. Polym.* **2016**, *142*, 189−198.

(17) Jiao, T.; Zhou, J.; Zhou, J. X.; Gao, L. H.; Xing, Y. Y.; Li, X. H. Synthesis and characterization of chitosan-based Schiff base compounds with aromatic substituent groups. *Iran. Polym. J.* **2011**, *20*, 123−136.

(18) Dolbow, J.; Fried, E.; Ji, H. Chemically induced swelling of hydrogels. *J. Mech. Phys. Solids* **2004**, *52*, 51−84.

(19) Naveen; Babu, S. A. Ring-closing metathesis reaction-based synthesis of new classes of polyether macrocyclic systems. *Tetrahedron* **2015**, *71*, 7758−7781.

(20) Mondal, R.; Mandal, T. K.; Mallik, A. K. Simple synthesis of a new family of 22- to 28-membered macrocycles containing two chalcone moieties. *ARKIVOC* **2012**, *9*, 9.

(21) Barba, V.; Ramos, P.; Jiménez, D.; Rivera, A.; Meneses, A. Calixarene and hemicarcer and-like compounds obtained by self-assembly of 3-aminophenylboronic acid and salicylaldehyde derivatives. *Inorg. Chim. Acta* **2013**, *401*, 30−37.

(22) Armstrong, L. G.; Lindoy, L. F. Studies involving nitrogen-oxygen donor macrocyclic ligands. I. nickel(II) complexes of a new series of cyclic ligands derived from salicylaldehyde. *Inorg. Chem.* **2002**, *14*, 1322−1326.

(23) Wang, J.; Wang, H. Preparation of soluble p-aminobenzoyl chitosan ester by Schiff's base and antibacterial activity of the derivatives. *Int. J. Biol. Macromol.* **2011**, *48*, 523−529.

(24) Yang, Z.; Shu, J.; Zhang, L.; Wang, Y. Preparation and adsorption behavior for metal ions of cyclic polyamine derivative of chitosan. *J. Appl. Polym. Sci.* **2006**, *100*, 3018−3023.

(25) Sun, Z.; Lv, F.; Cao, L.; Liu, L.; Zhang, Y.; Lu, Z. Multistimuli-Responsive, Moldable Supramolecular Hydrogels Cross-Linked by Ultrafast Complexation of Metal Ions and Biopolymers. *Angew. Chem., Int. Ed.* **2015**, *54*, 7944−7948.

DOI: 10.1021/acsomega.8b01872
ACS Omega 2018, 3, 17416−17424

(26) Trimukhe, K.; Varma, A. A morphological study of heavy metal complexes of chitosan and crosslinked chitosans by SEM and WAXRD. *Carbohydr. Polym.* **2008**, *71*, 698−702.
(27) Evmenenko, G.; Alexeev, V.; Budtova, T.; Buyanov, A.; Frenkel, S. Swelling-induced structure changes of polyelectrolyte gels. *Polymer* **1999**, *40*, 2975−2979.
(28) Karadag, E.; Saraydın, D. Swelling of superabsorbent acrylamide/sodium acrylate hydrogels prepared by using multi-functional cross-linkers. *Turk. J. Chem.* **2002**, *26*, 863−875.
(29) Rinaudo, M. Chitin and chitosan: Properties and applications. *Prog. Polym. Sci.* **2006**, *31*, 603−632.
(30) Sheldrick, G. M. *SHELX 97 Programs for the refinement of Crystal Structures*; University of Göttingen: Germany,1997.
(31) Brugnerotto, J.; Lizardi, J.; Goycoolea, F. M.; Argüelles-Monal, W.; Desbrières, J.; Rinaudo, M. An infrared investigation in relation with chitin and chitosan characterization. *Polymer* **2001**, *42*, 3569−3580.
(32) Demetgül, C. Synthesis of the ketimine of chitosan and 4,6-diacetylresorcinol, and study of the catalase-like activity of its copper chelate. *Carbohydr. Polym.* **2012**, *89*, 354−361.
(33) Heux, L.; Brugnerotto, J.; Desbrières, J.; Versali, M.-F.; Rinaudo, M. Solid state NMR for determination of degree of acetylation of chitin and chitosan. *Biomacromolecules* **2000**, *1*, 746−751.
(34) Otte, D. A. L.; Borchmann, D. E.; Lin, C.; Weck, M.; Woerpel, K. A. 13C NMR Spectroscopy for the Quantitative Determination of Compound Ratios and Polymer End Groups. *Org. Lett.* **2014**, *16*, 1566−1569.
(35) Koul, V.; Mohamed, R.; Kuckling, D.; Adler, H.-J. P.; Choudhary, V. Interpenetrating polymer network (IPN) nanogels based on gelatin and poly(acrylic acid) by inverse miniemulsion technique: Synthesis and characterization. *Colloids Surf., B* **2011**, *83*, 204−213.
(36) Demetgül, C.; Beyazit, N. Synthesis, characterization and antioxidant activity of chitosan-chromone derivatives. *Carbohydr. Polym.* **2018**, *181*, 812−817.
(37) Kumar, S.; Koh, J. Physiochemical, optical and biological activity of chitosan-chromone derivative for biomedical applications. *Int. J. Mol. Sci.* **2012**, *13*, 6102−6116.
(38) Wang, X.; Du, Y.; Fan, L.; Liu, H.; Hu, Y. Chitosan- metal complexes as antimicrobial agent: synthesis, characterization and structure-activity study. *Polym. Bull.* **2005**, *55*, 105−113.
(39) Wan, Y.; Creber, K. A. M.; Peppley, B.; Tam Bui, V. Ionic conductivity and tensile properties of hydroxyethyl and hydroxypropyl chitosan membranes. *J. Polym. Sci., Part B: Polym. Phys.* **2004**, *42*, 1379−1397.
(40) Franca, E. F.; Lins, R. D.; Freitas, L. C. G.; Straatsma, T. P. Characterization of chitin and chitosan molecular structure in aqueous solution. *J. Chem. Theory Comput.* **2008**, *4*, 2141−2149.
(41) Hong, P.-Z.; Li, S.-D.; Ou, C.-Y.; Li, C.-P.; Yang, L.; Zhang, C.-H. Thermogravimetric analysis of chitosan. *J. Appl. Polym. Sci.* **2007**, *105*, 547−551.
(42) Low, H. Y.; Ishida, H. Structural effects of phenols on the thermal and thermo-oxidative degradation of polybenzoxazines. *Polymer* **1999**, *40*, 4365−4376.
(43) Szycher, M. *Szycher's Handbook of Polyurethane*, 1st ed.; CRC Press, 1999; pp 3−31.
(44) Anirudhan, T. S.; Rijith, S. Glutaraldehyde cross-linked epoxyaminated chitosan as an adsorbent for the removal and recovery of copper(II) from aqueous media. *Colloids Surf., A* **2009**, *351*, 52−59.
(45) Cao, J.; Li, D.; Liang, W.; Wang, Y.; Wu, D. Glutaraldehyde Cross-Linked Chitosan Nanofibers: Preparation, Characterization and Application in Adsorption of Cu (II). *J. Nanosci. Nanotechnol.* **2016**, *16*, 2922−2928.
(46) Üzüm, Ö. B.; Karadağ, E. Dye sorption and water uptake properties of crosslinked acrylamide/sodium methacrylate copolymers and semi-interpenetrating polymer networks composed of PEG. *Sep. Sci. Technol.* **2011**, *46*, 489−499.
(47) Duman, S. S.; Şenel, S. Chitosan and its Applications in Veterinary Medicine. *J. Vet. Surg.* **2004**, *10*, 62−72.
(48) Saraydın, D.; Karadağ, E.; Isıkver, Y.; Şahiner, N.; Güven, O. The influence of preparation methods on the swelling and network properties of acrylamide hydrogels with crosslinkers. *J. Macromol. Sci., Part A: Pure Appl.Chem.* **2004**, *41*, 421−433.
(49) Karadağ, E.; Saraydın, D.; Güven, O. Water absorbency studies of γ-radiation crosslinked poly(acrylamide-co-2,3-dihydroxybutane-dioic acid) hydrogels. *Nucl. Instrum. Methods Phys. Res., Sect. B* **2004**, *225*, 489−496.

DOI: 10.1021/acsomega.8b01872
ACS Omega 2018, 3, 17416−17424